



Universiteit
Leiden
The Netherlands

Polymyxin stereochemistry and its role in antibacterial activity and outer membrane disruption

Slingerland, C.J.; Kotsogianni, A.I.; Wesseling, C.M.J.; Martin, N.I.

Citation

Slingerland, C. J., Kotsogianni, A. I., Wesseling, C. M. J., & Martin, N. I. (2022). Polymyxin stereochemistry and its role in antibacterial activity and outer membrane disruption. *Acs Infectious Diseases*, 8(12), 2396-2404. doi:10.1021/acsinfecdis.2c00307

Version: Publisher's Version

License: [Creative Commons CC BY 4.0 license](https://creativecommons.org/licenses/by/4.0/)

Downloaded from: <https://hdl.handle.net/1887/3515153>

Note: To cite this publication please use the final published version (if applicable).

Polymyxin Stereochemistry and Its Role in Antibacterial Activity and Outer Membrane Disruption

Cornelis J. Slingerland, Ioli Kotsogianni, Charlotte M. J. Wesseling, and Nathaniel I. Martin*



Cite This: *ACS Infect. Dis.* 2022, 8, 2396–2404



Read Online

ACCESS |



Metrics & More



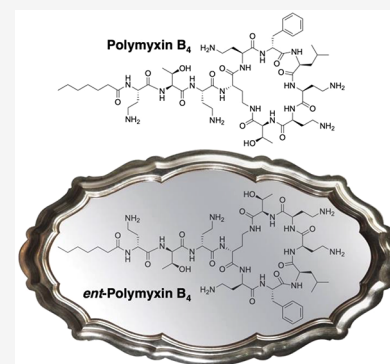
Article Recommendations



Supporting Information

ABSTRACT: With increasing rates of resistance toward commonly used antibiotics, especially among Gram-negative bacteria, there is renewed interest in polymyxins. Polymyxins are lipopeptide antibiotics with potent anti-Gram-negative activity and are generally believed to target lipid A, the lipopolysaccharide (LPS) anchor found in the outer membrane of Gram-negative bacteria. To characterize the stereochemical aspects of their mechanism(s) of action, we synthesized the full enantiomers of polymyxin B and the polymyxin B nonapeptide (PMBN). Both compounds were compared with the natural compounds in biological and biophysical assays, revealing strongly reduced antibacterial activity for the enantiomeric species. The enantiomeric compounds also exhibit reduced LPS binding, lower outer membrane (OM) permeabilization, and loss of synergistic potential. These findings provide new insights into the stereochemical requirements underlying the mechanisms of action of polymyxin B and PMBN.

KEYWORDS: *polymyxin B, polymyxin B nonapeptide, mechanism of action, stereochemistry, enantiomers*



Polymyxin antibiotics are a family of cyclic lipopeptides among which polymyxin B and polymyxin E (colistin) are used clinically (Figure 1A). Given their potent and specific anti-Gram-negative activity, the clinical application of polymyxins is on the rise as a result of global dissemination of multidrug resistant bacteria.^{1,2} Produced by the soil dwelling microorganism *Paenibacillus polymyxa*,^{3,4} polymyxins comprise a class of polycationic decapeptides carrying a lipophilic tail. Due to the presence of several nonproteogenic diamino butyric acid (Dab) residues, the peptide is polycationic at physiological pH. The decapeptide part consists of a seven-membered ring with three exocyclic residues connecting the ring to the N-terminal lipophilic tail.⁵ Polymyxins are typically obtained and clinically used as a mixture of closely related congeners.² While polymyxins B and E differ with respect to the amino acid at position 6 (D-Phe and D-Leu, respectively), minor variations are also found in the lipophilic acyl tail, as exemplified by the structures of polymyxins B₁ and B₄ (Figure 1A).⁵ Previous studies into polymyxin B and polymyxin E variants bearing slightly different lipid tails have shown them to display similar antibacterial activities.⁶

The primary mechanism by which the polymyxins target Gram-negative bacteria is by binding to lipid A,^{7–9} the membrane anchoring moiety of the lipopolysaccharide (LPS) comprising the outer membrane (OM) of Gram-negative cells. Lipid A is a structurally complex biomolecule composed of a disaccharide consisting of two phosphorylated glucosamine units that are decorated with a number of acyl tails that facilitate embedding in the OM (Figure 1B). Polymyxin

sensitivity and resistance is strongly dependent on the structural features of lipid A. Notably, many modified lipid A variants exist naturally, either in a species specific fashion or as the result of acquired resistance genes. For instance, *Neisseria gonorrhoeae* is intrinsically resistant to polymyxins as a result of the inclusion of a phosphoethanolamine moiety at the 4' position of the lipid A headgroup, which serves to reduce its binding by polymyxins.^{10,11} A similar lipid A modification is observed as a result of the recently reported plasmid-mediated, mobile colistin resistance (*mcr*) genes, which encode for phosphoethanolamine transferases that also modify the structure of lipid A at the 1' position and in doing so confer polymyxin resistance.^{12–14}

From a mechanistic perspective, the activity of the cationic polymyxins is ascribed to their electrostatic interactions with the negatively charged phosphate groups of lipid A, which leads to displacement of divalent cations that bridge adjacent phosphate containing molecules.^{2,9,15–17} As a result, “OM loosening” occurs, which in turn allows for polymyxin passage across the OM.^{17,18} With access to the periplasmic space, the polymyxins go on to exert their secondary effects on the cytoplasmic membrane.^{4,13} Interestingly, recent studies have

Received: June 13, 2022

Published: November 7, 2022



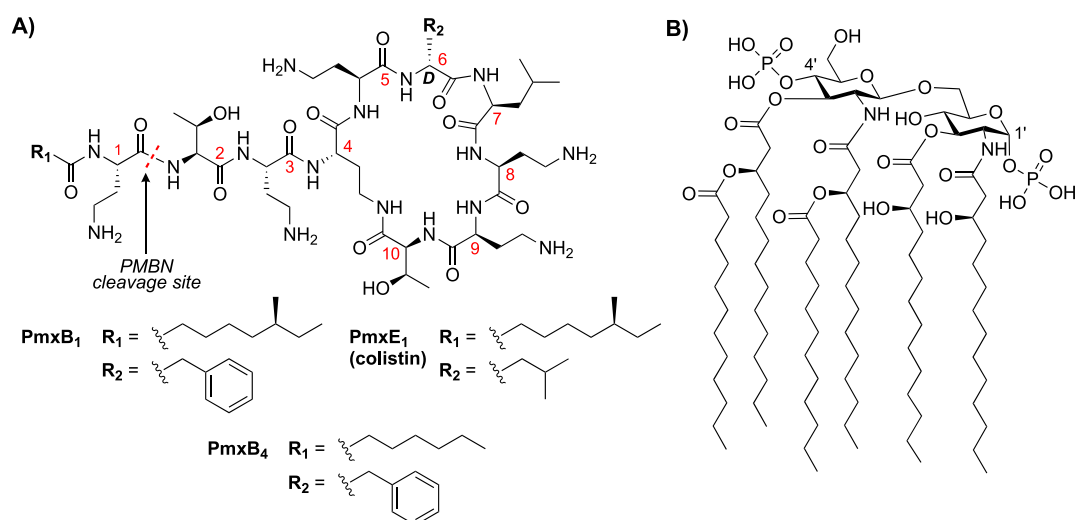
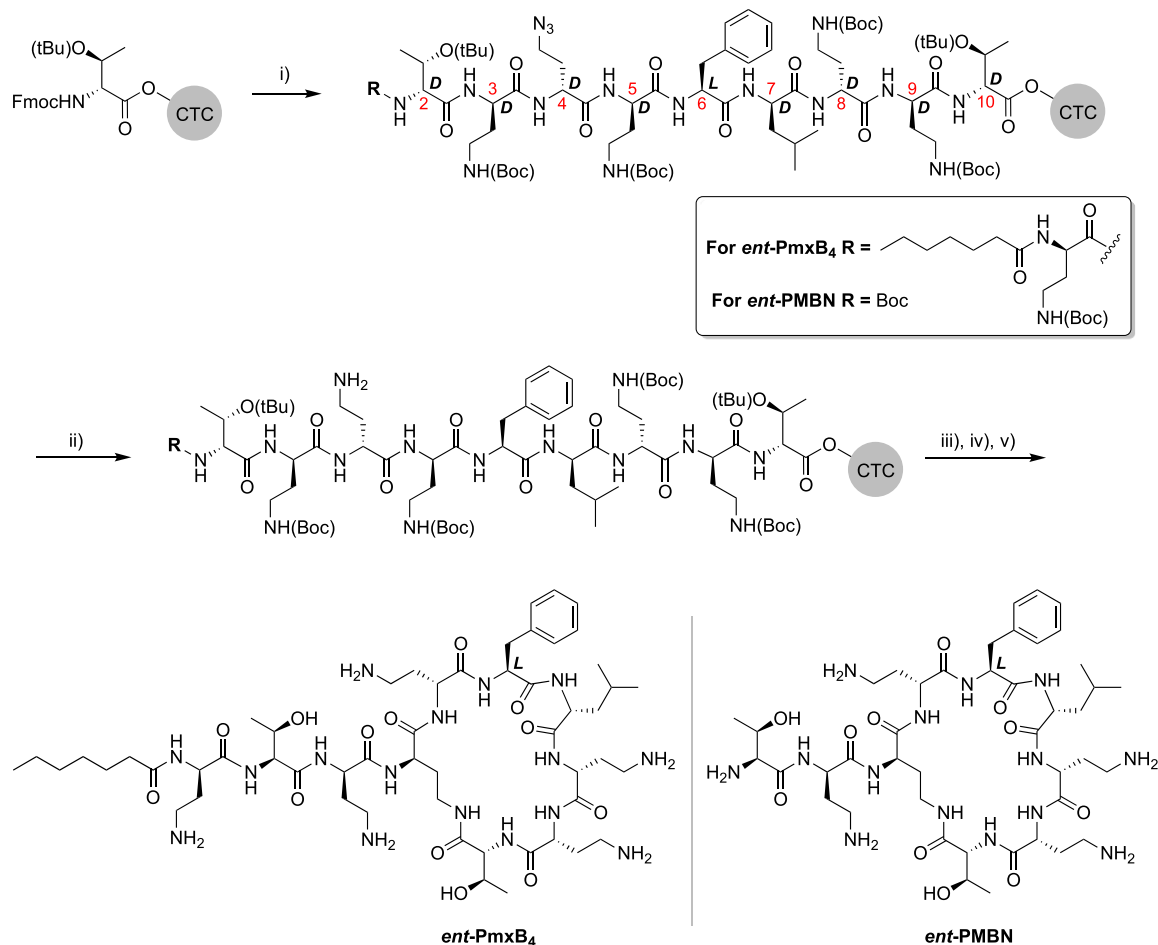


Figure 1. Polymyxins and their target lipid A. (A) Structures of clinically used polymyxin B and polymyxin E (colistin) including the numbering typically used for polymyxin residues. (B) Structure of lipid A (from *E. coli* K-12), the LPS membrane anchoring lipid in Gram-negative bacteria.

Scheme 1. Solid Phase Peptide Synthesis (SPPS) of Enantiomeric Polymyxin B4 (*ent*-PmxB4) and Enantiomeric Polymyxin B Nonapeptide (*ent*-PMBN)^a



^aReagents and conditions: (i) standard SPPS with 4 equiv of FmocAA (coupling: BOP/DIPEA, deprotection: 20% piperidine in DMF) to yield the resin-bound linear peptide intermediates; (ii) on-resin azide group reduction with DTT, DIPA, dry DMF, RT, 3 × 2 h; (iii) mild acid resin cleavage with HFIP/DCM (20/80), 1.5 h; (iv) solution-phase cyclization with DIC/Oxyma, DMF, o/n; (v) global deprotection with TFA, TIPS, H₂O.

also suggested that the bactericidal effect of the polymyxins is mediated by their engagement with nascent LPS present in the cytoplasmic membrane.¹⁹

It is also well established that the nonapeptide fragment obtained by enzymatic degradation of polymyxin B (Figure 1A) retains the OM disrupting abilities of the parent

compound despite lacking antibiotic activity. This finding has spurred a number of investigations into the use of polymyxin B nonapeptide (PMBN) as a synergist capable of potentiating the activity of antibiotics that typically cannot cross the Gram-negative OM.^{20–22} In addition, several studies describing the development of synthetic PMBN analogues as antibiotic adjuvants have been reported in recent years.^{23–25}

Structure–activity relationship studies aimed at elucidating the contribution of component amino acid stereochemistry to the activity of the polymyxins and PMBN have also been reported.^{26,27} In a recent study, the Raymond group generated a library of stereorandomized polymyxin B analogues that in some cases exhibited good-to-moderate activity against *E. coli*.²⁶ In addition, Fridkin and co-workers previously prepared and characterized the activity of the enantiomeric form of PMBN, showing it to be a much less active antibiotic synergist.²⁷ Absent from these prior studies, however, is an assessment of the completely mirror-image enantiomeric form of any full-length polymyxin. Such mirror-image strategies have been previously applied by our group and others to better understand the stereochemical parameters governing the mechanisms of various peptide antibiotics.^{28–32} In those cases where an achiral target is implicated, the enantiomeric form of the peptide antibiotic generally exhibits activity on par with the natural product. This is the case for laspartomycin, which targets undecaprenyl phosphate (C₅₅-P)³² as well as the clinically used bacitracin, which targets undecaprenyl pyrophosphate (C₅₅-PP).³¹ In contrast, for peptide antibiotics with an implicated chiral biomolecular target, the activity of the corresponding enantiomer is often significantly reduced. Specific examples include the recently reported laterocidine (targeting lipid A),³⁰ tridecaptin A1 (targeting the bacterial cell wall precursor lipid II),²⁹ thanatin (targeting LptA and LptD proteins involved in LPS biosynthesis),²⁸ and daptomycin (targeting phosphatidylglycerol).³³ In all of these examples, the antibacterial activity of the corresponding enantiomers was shown to be either severely decreased or abolished. Using a similar approach, we here describe the synthesis of enantiomeric polymyxin B₄ along with the corresponding PMBN enantiomer. The activities of the enantiomeric species were subsequently compared to their natural counterparts in a variety of biological and biophysical assays, providing new insights into the stereochemical requirements that govern the antibacterial mechanism of action of the polymyxins.

In considering which polymyxin to use for mirror image analysis, we selected polymyxin B₄ (PmxB₄, Figure 1A). Bearing a linear C7 lipid, PmxB₄ has been previously shown to have the same activity as polymyxin B₁⁶ with the C7 lipid offering the advantage of having one less stereogenic center to be concerned with when synthesizing the enantiomeric species. To date, a number of solid phase syntheses of polymyxin B have been reported.^{6,34,35} Inspired by these, both *ent*-PmxB₄ and *ent*-PMBN were synthesized using a combined solid- and solution-phase approach (Scheme 1). The protected linear peptide intermediates were assembled on a solid support using 2-chlorotrityl chloro (CTC) resin and the corresponding enantiomeric Fmoc amino acid building blocks starting from D-Thr10. As indicated in Scheme 1, the linear *ent*-PmxB₄ precursor was assembled to include the N-terminal Dab residue bearing the heptanoic acid moiety, while the *ent*-PMBN precursor peptide terminated with Boc-Thr. In both cases, an orthogonal protecting group strategy was required

for the amino side chain of the D-Dab residue at position 4 given its role in the subsequent ring closure. While previous reports have described the use of Alloc³⁵ or Mtt³⁴ protecting groups for this purpose, we found that using the corresponding azide was more practical. To this end, we incorporated Fmoc-D-Dab(N₃) at position 4 in the linear peptide intermediates. Once the linear peptides were assembled, the azide moiety of D-Dab(N₃) was cleanly reduced by treatment with DTT/DIPA in dry DMF.³⁶ After the reduction was deemed complete by LC/MS analysis, the protected peptides were cleaved from the resin by HFIP treatment and cyclized in solution. Using this strategy, both *ent*-PmxB₄ and PmxB₄, as well as *ent*-PMBN, were prepared using the appropriate D- or L-Fmoc-amino acids. In the case of PMBN with natural stereochemistry, we elected to use the well-established route wherein the parent natural product is enzymatically degraded using ficin.^{37,38} HPLC analysis and HRMS analysis (Table S1, Figures S1 and S2) confirmed the identity and expected equivalence of *ent*-PmxB₄ to PmxB₄ and *ent*-PMBN to PMBN and *ent*-PMBN. In addition and as expected, the obtained high field NMR spectra (¹H and 2D NOESY) were found to be identical for the enantiomeric pairs (Figures S3–S6).

We next evaluated the activity of both PmxB₄ and *ent*-PmxB₄ against several strains of Gram-negative bacteria (Tables 1 and S2). While PmxB₄ was found to exhibit low minimal inhibitory concentration (MIC) values in line with the clinically used polymyxin B, this was clearly not the case for *ent*-PmxB₄ as the enantiomeric species was found to be devoid of activity. Only at the highest concentration tested of 128 μg/mL was the growth of the *E. coli* strains impacted, while for *K. pneumoniae*, *A. baumannii*, and *P. aeruginosa*, no activity was observed. The addition of known OM disrupting agents like PMBN or the PMBN derivative SPR741³⁹ also did not improve the activity of *ent*-PmxB₄ (Table S3). Also of note, while *E. coli* strains with severely truncated LPS (as in the ΔwaaD and ΔwaaC mutants) were found to have increased sensitivity to PmxB₄, the activity of *ent*-PmxB₄ was not enhanced (Table 1). These results show that the full LPS structure is not required for the action of PmxB₄, a finding supportive of the recent suggestion that the core

Table 1. Minimal Inhibitory Concentration (MIC) Values for PmxB₄ and *ent*-PmxB₄^a

	strain	PmxB ₄	<i>ent</i> -PmxB ₄	PmxB (commercial)
<i>E. coli</i>	ATCC 25922	0.25	128	1
	BW25113	0.5	>128	1
	<i>mcr</i> -1	4	128	4
	JW3594 (ΔwaaD)	0.06	128	0.06
	JW3596 (ΔwaaC)	0.06	128	0.06
	<i>K. pneumoniae</i> ATCC 13883	0.125	>128	0.25
<i>A. baumannii</i> ATCC 19606	0.5	>128	0.25	
<i>P. aeruginosa</i>	ATCC 27853	0.25	>128	1
	NRZ03961	0.25	>128	1
	ATCC 10145	0.25	>128	1
	2018-007	0.5	>128	2

^aMIC values are derived from triplicate experiments and are expressed as μg/mL. See Figure S7 for the analysis of PmxB obtained from commercial sources.

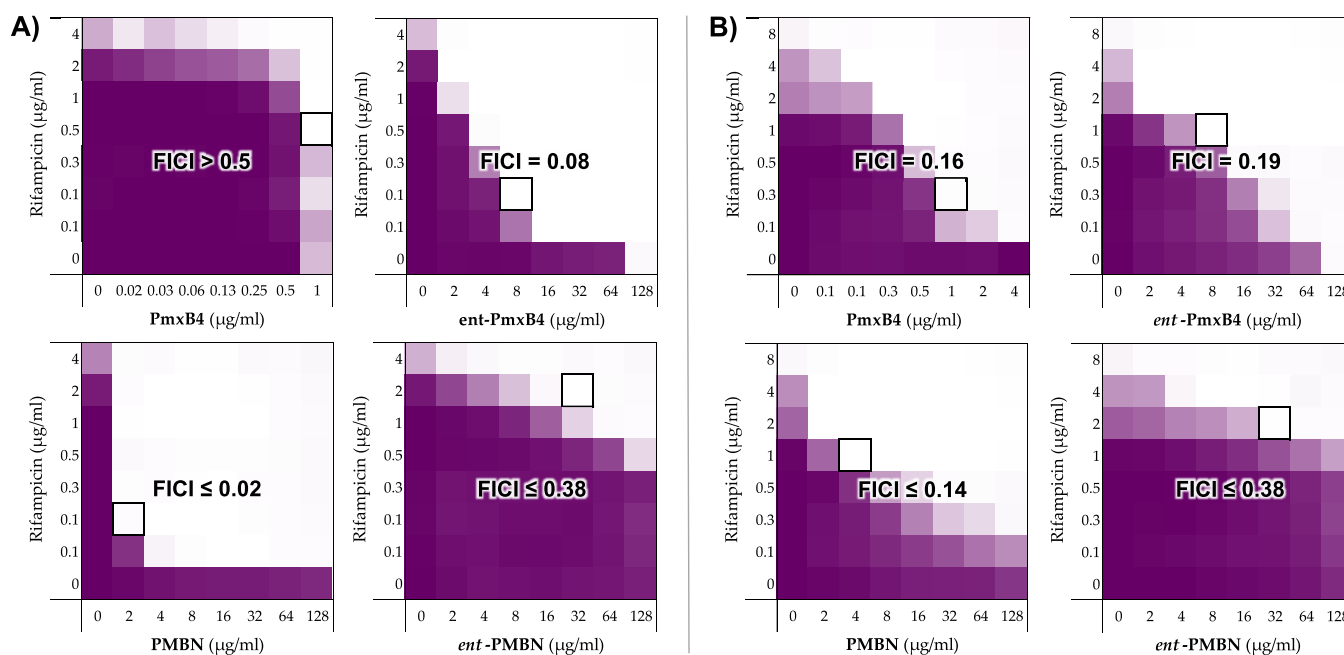


Figure 2. Analysis of rifampicin potentiation by enantiomeric pairs PmxB₄/ent-PmxB₄ and PMBN/ent-PMBN against polyxymyxin-sensitive and polyxymyxin-resistant bacteria. (A) Checkerboard assays to assess the synergy of rifampicin with PmxB₄/ent-PmxB₄ and PMBN/ent-PMBN against polyxymyxin-sensitive *E. coli* ATCC 25922. (B) Checkerboard assays to assess the synergy of rifampicin with PmxB₄/ent-PmxB₄ and PMBN/ent-PMBN against polyxymyxin-resistant (*mcr-1* positive) *E. coli*. Color corresponds to growth (as read by OD₆₀₀) after incubation and with intensity proportional to the observed OD₆₀₀ value. White areas indicate no growth. Bounded box indicates the combination of concentrations that gives the lowest FICI index value. Values used for FICI calculations are shown in Table S4.

sugars of LPS might in fact lower the efficacy of polyxymyxin antibiotics by hindering them from reaching lipid A.⁴⁰ In contrast, the absence of a complete LPS layer did not serve to enhance the activity of ent-PmxB₄, further demonstrating the high degree of stereospecificity that underpins the antibacterial mechanism of the polyxymyxins.

Having established that ent-PmxB₄ is devoid of inherent antibacterial activity, we next turned our attention to evaluating its potential as an antibiotic synergist. The rationale for doing so was inspired by a recent report from Brown and co-workers who found that, when tested against polyxymyxin-resistant (*mcr*-positive) strains, polyxymyxins exhibit synergistic activity with Gram-positive specific antibiotics like rifampicin.⁴¹ This is notable in that it suggests that, while strong lipid A binding is needed for antibacterial activity, it is not a prerequisite for synergistic activity. Also of note is another study, again from the Brown group, which revealed that PMBN loses its synergistic activity against *mcr*-positive strains, implying that the lipid tail in full-length polyxymyxins is needed to maintain synergy against polyxymyxin-resistant bacteria.⁴² To this end, we performed a series of checkerboard assays to assess the capacity of the enantiomeric pairs PmxB₄ and ent-PmxB₄ as well as PMBN and ent-PMBN to potentiate the activity of rifampicin against both polyxymyxin-sensitive and polyxymyxin-resistant strains (Figure 2).

Given the potent inherent antimicrobial activity of polyxymyxin antibiotics, they are not typically examined for synergism with other antibiotics. In keeping with this and as illustrated in Figure 2A, PmxB₄ is not an effective synergist of rifampicin against polyxymyxin-sensitive *E. coli* due largely to its already low MIC (2 μg/mL) against the strain used. In contrast, ent-pmxB₄ shows a very clear synergistic effect with rifampicin. Specifically, while ent-PmxB₄ alone has a very high

MIC of 128 μg/mL, when administered at 8 μg/mL, it very effectively lowers the MIC of rifampicin from 8 to 0.1 μg/mL, corresponding to a calculated FICI value of 0.075. In contrast, when comparing the synergistic activity of PMBN and ent-PMBN, the opposite trend is observed. It is well established that, despite lacking the inherent antimicrobial activity of the parent lipopeptide, PMBN is a potent synergist of many antibiotics, including rifampicin, that are generally only used to treat Gram-positive infections.^{43,24} In this regard and as expected, our assessment of the effect of PMBN on the activity of rifampicin against polyxymyxin-sensitive *E. coli* revealed a strong synergistic effect with a corresponding calculated FICI value of 0.020. In comparison and as readily seen from the checkerboard data, only a minor potentiation of rifampicin is achieved by ent-PMBN, requiring high concentrations and corresponding to an FICI value of 0.375. These findings are in agreement with the previous studies of Fridkin and co-workers who found ent-PMBN to also be a poor potentiator of novobiocin and erythromycin.²⁷ We next examined the synergistic activity of rifampicin with the PmxB₄/ent-PmxB₄ and PMBN/ent-PMBN enantiomeric pairs in the context of an *mcr-1* positive *E. coli* strain (Figure 2B). Of particular note is the finding that in this case PmxB₄ and ent-PmxB₄ exhibit a similarly moderate degree of synergy with FICI values of 0.163 and 0.188, respectively. In the case of PMBN, the synergistic activity is heavily impacted compared to the polyxymyxin-sensitive strain, resulting in an increased FICI value of 0.141, while for ent-PMBN, the same low level of synergy was found (FICI 0.375). Taken together, these findings support the idea that, in the absence of specific lipid A binding, an effective synergist likely needs to be both polycationic in nature and include a membrane-anchoring hydrophobic moiety.

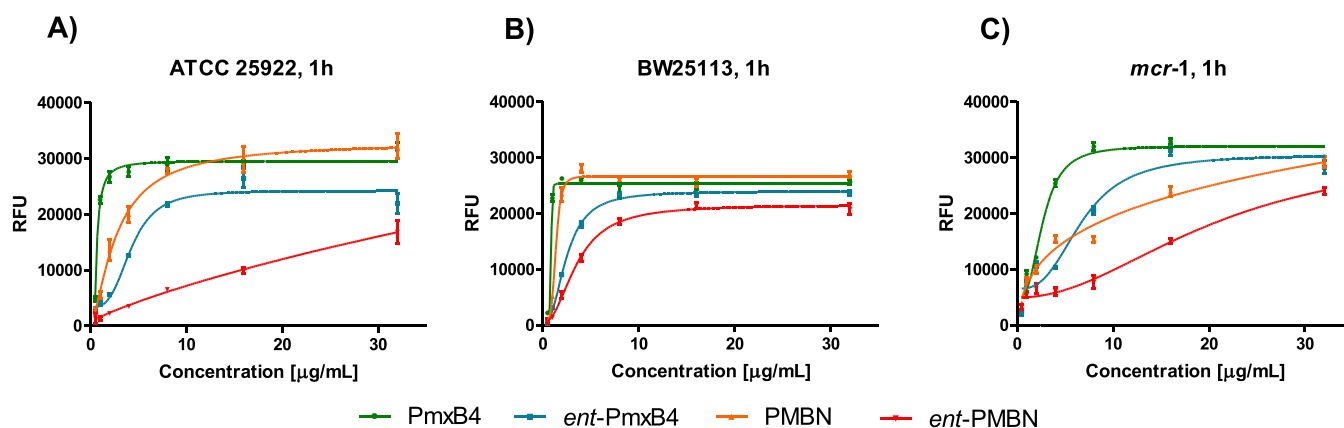


Figure 3. *N*-Phenyl-1-naphthyl (NPN) uptake in *E. coli* upon incubation with PmxB₄/ent-PmxB₄ and PMBN/ent-PMBN. (A, B) NPN uptake in polymyxin-sensitive strains ATCC 25922 (smooth LPS) and BW25113 (rough LPS); (C) NPN uptake in the polymyxin-resistant, *mcr-1* positive strain. Values and associated error bars are based on triplicates with fluorescence read-out after 1 h of incubation. RFU: relative fluorescence unit.

We next investigated the role of OM perturbation in the observed potentiation of rifampicin by PmxB₄/ent-PmxB₄ and PMBN/ent-PMBN. To do so, we applied a well-established fluorescence-based assay that reports the uptake of *N*-phenyl-1-naphthylamine (NPN). Only upon OM disruption can the hydrophobic NPN gain access to the phospholipid layer, resulting in an increase in fluorescence.⁴⁴ Previous studies have validated this assay for assessing the relative activity of OM disrupting agents, most notably PMBN, which causes a clear increase in fluorescence when added to Gram-negative bacteria in the presence of NPN.^{16,22} For our investigations, we characterized the OM perturbation of three different *E. coli* strains: two polymyxin-sensitive strains containing either smooth LPS (ATCC 25922) or rough LPS (BW25113) (Figure 3A,B) and one polymyxin-resistant strain containing phosphoethanolamine modified LPS (*mcr-1* positive) (Figure 3C).

As seen in Figure 3A,B, against the polymyxin-sensitive *E. coli* strains tested, both PmxB₄ and PMBN were found to elicit potent OM disruption with PMBN acting more effectively on the rough LPS strain BW25113. In comparison, ent-PmxB₄ was found to induce moderate OM disruption against both polymyxin-sensitive strains. Interestingly, while ent-PMBN showed only weak OM disruption against the *E. coli* strain ATCC 25922 containing smooth LPS, against the BW25113 strain (containing rough LPS), a higher degree of OM perturbation was observed. These findings indicate that in general the rough LPS containing BW25113 strain appears to have a greater sensitivity to OM disruption based on the NPN assay. In line with the results of the synergy studies, against the *mcr*-positive *E. coli* strain, higher concentrations of all four compounds were required to achieve NPN uptake (Figure 3C). In this case, PmxB₄ elicits the most effective OM disruption with ent-PmxB₄ also achieving full NPN uptake albeit at higher concentrations. In comparison, both PMBN and ent-PmxB₄ failed to achieve full NPN uptake at the highest concentration tested of 32 μg/mL. Taken together, these data again support the conclusion that, in developing OM disrupting agents with activity against strains bearing structurally modified lipid A, the presence of a lipophilic moiety is essential.

We also used isothermal titration calorimetry (ITC) to study target engagement by PmxB₄/ent-PmxB₄ and PMBN/

ent-PMBN (Figure 4). Previous reports using ITC to characterize the interaction of polymyxins with LPS have revealed it to be a complex process that is highly dependent on the source of the LPS and the experimental conditions used.^{9,45–47} For our investigations, we elected to use a commercially available LPS preparation (derived from *E. coli* O55:B5) that has also been used previously for ITC studies aimed at assessing binding interactions with polymyxins.⁴⁵ We found that titration of the polymyxin analogues (1 mM solution) into the sample cell containing LPS (at an estimated concentration of 20 μM) gave the most reproducible results. An exothermic interaction was observed upon titration of PmxB₄ into the LPS solution (Figure 4A), while titration of PmxB₄ into buffer alone yielded no signal (Figure S9), indicating that the heat measured derives from interactions with LPS. In agreement with previous reports, the thermograms resulting from the titration of PmxB₄ into the LPS solution are complex and do not fit a one-step binding process.^{45,46} For this reason, a simple dissociation constant cannot be reliably determined for the interaction. In addition, because the LPS used is a complex mixture, an estimate of its molecular weight (20 kDa) was applied, which in turn precludes a precise determination of the molar ratios for the binding of LPS by the polymyxins here studied. It is, however, possible to compare the relative enthalpies of LPS binding for the different polymyxins along with the shapes of the resulting binding thermograms. The thermogram obtained upon titration of ent-PmxB₄ into LPS shows a different pattern than that observed for the titration with PmxB₄ (Figure 4A, upper right). While an exothermic interaction was still observed, the corresponding Δ*H* is much smaller (Figure 4B), indicating a less productive interaction with LPS. In addition, saturation took longer to achieve, suggesting that more equivalents are needed to occupy the available binding sites on the LPS. Interestingly, for PMBN and ent-PMBN, the thermograms are quite similar, both showing saturation at about 70 min (Figure 4A bottom) with a slightly smaller Δ*H* measured for the enantiomeric species. These data suggest that, despite PMBN being a vastly superior OM disrupting agent and antibiotic synergist compared to ent-PMBN, both appear to interact with LPS in a similar manner. Notably, this finding is in agreement with previous studies where PMBN and ent-PMBN were found to have comparable LPS

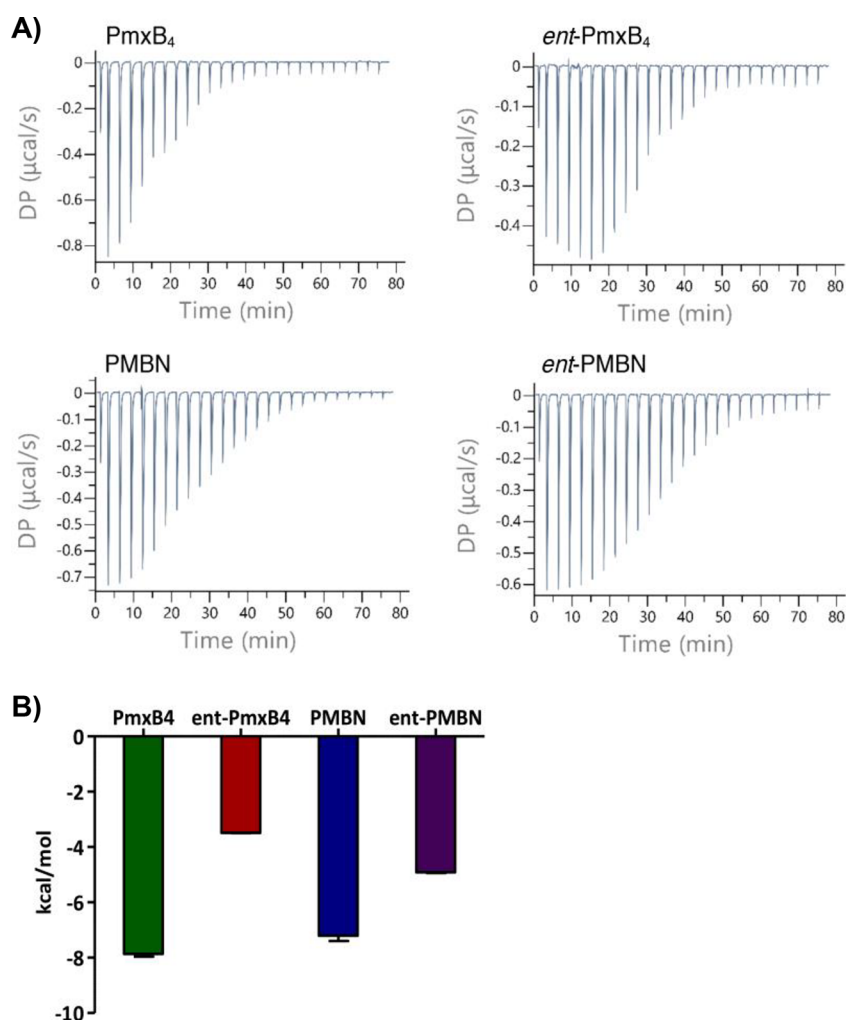


Figure 4. ITC experiments to assess LPS binding by PmxB₄/ent-PmxB₄ and PMBN/ent-PMBN. (A) Representative thermograms resulting from titration of the polymyxin peptide indicated (1 mM) into the LPS solution (20 μM). (B) Observed enthalpy change upon titration of peptide into LPS. All experiments were run in triplicate; full data provided in Figures S8–S14 and Table S5.

interactions based on their capacities to similarly displace dansyl-labeled PMBN from intact *E. coli*.²⁷

In summary, we here report a robust synthetic route for the production of polymyxins and have applied it in the preparation of PmxB₄ along with its novel enantiomer ent-PmxB₄. Antibacterial assays show that, while PmxB₄ is a potent anti-Gram-negative antibiotic, ent-PmxB₄ is devoid of activity. Moreover, the enantiomer of PMBN, ent-PMBN, was also synthesized and found to exhibit a reduced potential, relative to PMBN, to synergize with antibiotics that are typically unable to pass the Gram-negative OM. These findings show that stereochemically defined target recognition is required for both the antibacterial action of full-length polymyxin antibiotics as well as the synergistic activity of the corresponding nonapeptides. Interestingly, despite the absence of inherent antibacterial activity, ent-PmxB₄ does cause OM disruption as evidenced by both its synergistic activity and ability to induce NPN uptake in live bacteria, including a polymyxin-resistant strain. Calorimetric investigations also revealed that, while PmxB₄ and ent-PmxB₄ both interact with LPS, binding by PmxB₄ is more efficient. The finding that ent-PmxB₄ and ent-PMBN do interact with LPS, albeit to a lower degree, suggests that, in the absence of precise target recognition, OM binding can still occur, most likely promoted

by electrostatic interactions. To conclude, our study is the first to characterize the antibacterial activity of the enantiomer of a full-length polymyxin and clearly reveals the essential stereospecificity of the mechanism of action behind these clinically important antibiotics.

METHODS

Peptide Synthesis. PmxB₄ and ent-PmxB₄. Fmoc-Thr(tBu) was loaded onto chlorotriyl resin via its carboxylic acid. Resin loading was determined to be 0.58 mmol·g⁻¹. The linear peptide encompassing the residues p10–p1 was assembled on resin using standard solid phase peptide synthesis (SPPS) conditions using a 4:4:8 ratio of amino acid:BOP:DIPEA relative to the resin. Typical coupling times were 1 h. For coupling of Fmoc-Dab(N3), 2 equiv of amino acid and BOP were used, and coupling time was extended to 4 h. Couplings were done in DMF, and deprotection was achieved using 20% piperidine in DMF (v/v). Amino acids were protected as follows: Boc for Fmoc-Dab, tBu for Fmoc-Thr, and N3 for Fmoc-Dab at p4. For PmxB₄, all L-amino acids were used, except for D-Phe at p6. For ent-PmxB, all D-amino acids were used, except for L-Phe at p6. After coupling heptanoic acid, the resin was washed well (DMF) and subjected to reduction of the Dab(N3) by a mixture of di-

isopropyl amine (DIPA) and dithiothreitol (DTT, racemic variant works well) in dry DMF (3 mL) for 2 h. Reduction was repeated twice. After washings, the peptide was cleaved from the resin by HFIP/DCM (20%, v/v) and cyclized overnight in 100 mL of DMF with DIC (3 equiv) and Oxyma Pure (6 equiv). After completion of cyclization, the mixture was concentrated and subjected to deprotection (TFA/TIPS/H₂O, 95/2.5/2.5) for 1.5 h. Deprotected peptide was crashed out in ice-cold MTBE and washed with MTBE, followed by lyophilization from *t*-BuOH/H₂O. Pure material was obtained after RP-HPLC purification (20–50% B gradient).

ent-PMBN. *ent*-PMBN was synthesized in a similar way as *ent*-PmxB4. After coupling Dab at p3, Boc-D-Thr(*t*Bu) was used as the final amino acid. The rest of the procedure is identical to that of *ent*-PmxB4.

PMBN. PMBN was synthesized from polymyxin B with slight modifications of previously described methods³⁷ as follows: Polymyxin B sulfate (commercially available mixture of isomers, Combi-Blocks, San Diego, USA, 4.0 g, 2.8 mmol) was dissolved in demiwater (120 mL). Dithiothreitol (DTT, 106 mg, 0.69 mmol) was added to the solution, followed by ficin (1.06 g, ~44 μmol). Enzymatic digestion was run at 37 °C under N₂ atmosphere overnight. Reaction progress was monitored by LC-MS. Additional dithiothreitol (16 mg, 63 μmol) and ficin (160 mg) were added, and digestion was run overnight once more. Once complete, the mixture was heated to reflux for 20 min, followed by filtration of the precipitate. The pH of the filtrate was adjusted to pH 2, and the sample was extracted with *n*-butanol (4 × 35 mL). The aqueous layer was freeze-dried from *t*-BuOH/H₂O. RP-HPLC was used to obtain pure PMBN (0–40% gradient).

MIC Experiments. MICs of compounds were determined following CLSI guidelines using the microbroth dilution method in polypropylene plates. Selected Gram-negative bacterial strains (see Table S2 for strain sources) were taken from glycerol stocks and grown overnight on blood agar. Individual colonies were selected and grown in Tryptic Soy Broth (TSB) to an OD₆₀₀ of 0.5. Compounds were diluted in Mueller Hinton Broth (MHB) supplemented with Mg²⁺ and Ca²⁺ at final concentrations of 12 and 20 mg/L, respectively (CAMHB). 50 μL was used for each well, and compounds were assessed in triplicates. Bacterial culture was diluted in CAMHB to 10⁶ CFU/mL, yielding 5 × 10⁵ CFU/mL upon addition of 50 μL of culture to 50 μL of compound solution. Positive and negative (sterility) controls were present on each plate. Plates were sealed with a semipermeable membrane and incubated for 22 h (*A. baumannii*) or 18 h (other strains) under shaking at 37 °C. MICs are defined as the lowest concentration of compound that visibly inhibits bacterial growth.

Checkerboard Assays. Selected Gram-negative bacterial strains were taken from glycerol stocks and grown overnight on blood agar. A single colony was inoculated in TSB broth at 37 °C until an optical density of 0.5 at 600 nm (OD₆₀₀) was reached. The bacterial suspension was diluted in freshly prepared CAMHB to 10⁶ CFU/mL. Compounds were diluted along the plate, using 25 μL of CAMHB for each dilution. Antibiotic concentrations were prepared separately in a multiwell reservoir, including a control without antibiotic. Of each antibiotic stock, 25 μL was added to three columns to obtain triplicates for every condition. To each 50 μL containing well was then added 50 μL of the 10⁶ CFU/mL bacterial suspension, and the plates were sealed with

breathable seals. After incubation for 18 h at 37 °C while shaking, the seals were removed and the density of the bacterial suspensions was measured at 600 nm (OD₆₀₀) using a Tecan Spark plate reader. The OD₆₀₀ values were transformed to a 2D gradient with the negative control as the minimum and the positive control as the maximum. The FICI was calculated using the following equation:

$$\text{FICI} = \frac{\text{MSC}_{\text{ant}}}{\text{MIC}_{\text{ant}}} + \frac{\text{MSC}_{\text{comp}}}{\text{MIC}_{\text{comp}}}$$

with MSC_{ant} and MSC_{comp} indicating the optimal synergistic concentration of antibiotic and compound and MIC_{ant} and MIC_{comp}, the corresponding MICs of the individual compounds. An FICI ≤ 0.5 indicates synergy.⁴⁸

NPN Assay. Bacteria were taken from glycerol stocks and grown in TSB overnight. Cultures were diluted either 50 or 100 times in Lysogeny Broth (LB) and grown at 37 °C to an OD₆₀₀ of 0.5. Test compounds were prepared in HEPES buffer (5 mM, pH 7.2 + 20 mM glucose) and serially diluted (25 μL per well) on 1/2 the area of black 96-well plates with a transparent bottom. *N*-Phenyl-1-naphthylamine (NPN) was dissolved in acetone (0.5 mM) and diluted to 40 μM in HEPES buffer (5 mM, pH 7.2 + 20 mM glucose). 25 μL of the NPN solution was added to each well. The bacterial suspension was spin down (1000g, 10 min), and the remaining cell pellet was resuspended in half the original volume of HEPES buffer (5 mM, pH 7.2 + 20 mM glucose). 50 μL of bacterial suspension was added to each well. NPN fluorescence was measured after 1 h of incubation at RT with λ_{ex} 355 ± 20 nm and λ_{em} 420 ± 20 nm. The measured fluorescence signal was corrected for NPN fluorescence in the absence of compounds (bacteria in buffer + NPN) and presented as relative fluorescence units (RFUs).

Isothermal Titration Calorimetry (ITC). Stock solutions of LPS (10 mg/mL, 0.5 mM) were prepared in 20 mM HEPES at pH 7 by suspension, sonication, and temperature cycling between 4 and 60 °C and stored overnight prior to use. LPS from *E. coli* (O55:B5) was used. Lipopeptide solutions (1 mM in 20 mM HEPES, pH 7) were titrated into a suspension of LPS (0.020 mM) in the same buffer. Control titrations included the titration of peptide into buffer and buffer into the LPS suspension to determine the corresponding heat of dilution. All binding experiments were performed using a MicroCal PEAQ-ITC Automated microcalorimeter (Malvern Panalytical Ltd., Malvern, UK). The samples were equilibrated to 37 °C prior to measurement. The titrations were conducted at 37 °C under constant stirring at 750 rpm. Each experiment consisted of an initial injection of 0.3 μL followed by 25 separate injections of 1.5 μL into the sample cell of 200 μL. The time between each injection was 180 s, and the measurements were performed with the reference power set at 5 μcal s⁻¹ and the feedback mode set at “low”. For all calculations performed, an estimated molecular weight of 20 kDa for LPS was applied. The calorimetric data thus obtained were analyzed using MicroCal PEAQ-ITC Analysis Software Version 1.20 (Malvern Panalytical Ltd., Malvern, UK), where the integrated heat signal is corrected for the heat of dilution of the titrant.

■ ASSOCIATED CONTENT

SI Supporting Information

The Supporting Information is available free of charge at <https://pubs.acs.org/doi/10.1021/acsinfecdis.2c00307>.

Abbreviations, reagents and general procedures, HRMS data, HPLC traces, and 1D and 2D NMR spectra for all peptides synthesized, information on bacterial strains, additional MIC analyses and FICI calculations, and ITC thermograms for all binding experiments performed (PDF)

■ AUTHOR INFORMATION

Corresponding Author

Nathaniel I. Martin – Biological Chemistry Group, Institute of Biology Leiden, Leiden University, 2333 BE Leiden, The Netherlands; orcid.org/0000-0001-8246-3006;
Email: n.i.martin@biology.leidenuniv.nl

Authors

Cornelis J. Slingerland – Biological Chemistry Group, Institute of Biology Leiden, Leiden University, 2333 BE Leiden, The Netherlands; orcid.org/0000-0003-0027-7491

Ioli Kotsogianni – Biological Chemistry Group, Institute of Biology Leiden, Leiden University, 2333 BE Leiden, The Netherlands; orcid.org/0000-0003-0078-0206

Charlotte M. J. Wesseling – Biological Chemistry Group, Institute of Biology Leiden, Leiden University, 2333 BE Leiden, The Netherlands

Complete contact information is available at:

<https://pubs.acs.org/10.1021/acsinfecdis.2c00307>

Notes

The authors declare no competing financial interest.

■ ACKNOWLEDGMENTS

The authors gratefully acknowledge Paolo Innocenti for performing HRMS analyses and Karthick Sai Sankar Gupta for assistance in acquiring NMR spectra. Financial support was provided by the European Research Council (ERC consolidator grant to N.I.M., grant agreement no. 725523).

■ REFERENCES

- (1) Bergen, P. J.; Landersdorfer, C. B.; Lee, H. J.; Li, J.; Nation, R. L. "Old" Antibiotics for Emerging Multidrug-Resistant Bacteria. *Curr. Opin. Infect. Dis.* **2012**, *25* (6), 626–633.
- (2) Velkov, T.; Thompson, P. E.; Nation, R. L.; Li, J. Structure–Activity Relationships of Polymyxin Antibiotics. *J. Med. Chem.* **2010**, *53* (5), 1898–1916.
- (3) Ash, C.; Priest, F. G.; Collins, M. D. Molecular Identification of rRNA Group 3 Bacilli (Ash, Farrow, Wallbanks and Collins) Using a PCR Probe Test. *Antonie Van Leeuwenhoek* **1994**, *64* (3), 253–260.
- (4) Trimble, M. J.; Mlynářčik, P.; Kolář, M.; Hancock, R. E. W. Polymyxin: Alternative Mechanisms of Action and Resistance. *Cold Spring Harb. Perspect. Med.* **2016**, *6* (10), a025288.
- (5) Brown, P.; Dawson, M. J. Development of New Polymyxin Derivatives for Multi-Drug Resistant Gram-Negative Infections. *J. Antibiot. (Tokyo)*. **2017**, *70* (4), 386–394.
- (6) Cui, A. L.; Hu, X. X.; Gao, Y.; Jin, J.; Yi, H.; Wang, X. K.; Nie, T. Y.; Chen, Y.; He, Q.-Y.; Guo, H. F.; Jiang, J. D.; You, X. F.; Li, Z. R. Synthesis and Bioactivity Investigation of the Individual Components of Cyclic Lipopeptide Antibiotics. *J. Med. Chem.* **2018**, *61* (5), 1845–1857.
- (7) Morrison, D. C.; Jacobs, D. M. Binding of Polymyxin B to the Lipid A Portion of Bacterial Lipopolysaccharides. *Immunochemistry* **1976**, *13* (10), 813–818.
- (8) Yin, N.; Marshall, R. L.; Matheson, S.; Savage, P. B. Synthesis of Lipid A Derivatives and Their Interactions with Polymyxin B and Polymyxin B Nonapeptide. *J. Am. Chem. Soc.* **2003**, *125* (9), 2426–2435.
- (9) Brandenburg, K.; David, A.; Howe, J.; Koch, M. H. J.; Andrä, J.; Garidel, P. Temperature Dependence of the Binding of Endotoxins to the Polycationic Peptides Polymyxin B and Its Nonapeptide. *Biophys. J.* **2005**, *88* (3), 1845–1858.
- (10) Kandler, J. L.; Joseph, S. J.; Balthazar, J.; Dhulipala, V.; Read, T. D.; Jerse, A. E.; Shafer, W. M. Phase-Variable Expression of LptA Modulates the Resistance of *Neisseria gonorrhoeae* to Cationic Antimicrobial Peptides. *Antimicrob. Agents Chemother.* **2014**, *58* (7), 4230–4233.
- (11) Jen, F. E. C.; Everest-Dass, A. V.; El-Deeb, I. M.; Singh, S.; Haselhorst, T.; Walker, M. J.; von Itzstein, M.; Jennings, M. P. *Neisseria gonorrhoeae* Becomes Susceptible to Polymyxin B and Colistin in the Presence of PBT2. *ACS Infect. Dis.* **2020**, *6* (1), 50–55.
- (12) Liu, Y. Y.; Wang, Y.; Walsh, T. R.; Yi, L. X.; Zhang, R.; Spencer, J.; Doi, Y.; Tian, G.; Dong, B.; Huang, X.; Yu, L. F.; Gu, D.; Ren, H.; Chen, X.; Lv, L.; He, D.; Zhou, H.; Liang, Z.; Liu, J. H.; Shen, J. Emergence of Plasmid-Mediated Colistin Resistance Mechanism MCR-1 in Animals and Human Beings in China: A Microbiological and Molecular Biological Study. *Lancet Infect. Dis.* **2016**, *16* (2), 161–168.
- (13) Ma, G.; Zhu, Y.; Yu, Z.; Ahmad, A.; Zhang, H. High Resolution Crystal Structure of the Catalytic Domain of MCR-1. *Sci. Rep.* **2016**, *6* (1), 39540.
- (14) Hussein, N. H.; AL-Kadmy, I. M. S.; Taha, B. M.; Hussein, J. D. Mobilized Colistin Resistance (*mcr*) Genes from 1 to 10: A Comprehensive Review. *Mol. Biol. Rep.* **2021**, *48* (3), 2897–2907.
- (15) Pristovšek, P.; Kidrič, J. Solution Structure of Polymyxins B and E and Effect of Binding to Lipopolysaccharide: An NMR and Molecular Modeling Study. *J. Med. Chem.* **1999**, *42* (22), 4604–4613.
- (16) Akhoundsadegh, N.; Belanger, C. R.; Hancock, R. E. W. Outer Membrane Interaction Kinetics of New Polymyxin B Analogs in Gram-Negative Bacilli. *Antimicrob. Agents Chemother.* **2019**, *63* (10), e00935-19.
- (17) Wiese, A.; Münstermann, M.; Gutschmann, T.; Lindner, B.; Kawahara, K.; Zähringer, U.; Seydel, U. Molecular Mechanisms of Polymyxin B-Membrane Interactions: Direct Correlation Between Surface Charge Density and Self-Promoted Transport. *J. Membr. Biol.* **1998**, *162* (2), 127–138.
- (18) Hancock, R. E. W. Peptide Antibiotics. *Lancet* **1997**, *349* (9049), 418–422.
- (19) Sabnis, A.; Hagart, K. L. H.; Klöckner, A.; Becce, M.; Evans, L. E.; Furniss, R. C. D.; Mavridou, D. A. I.; Murphy, R.; Stevens, M. M.; Davies, J. C.; Larrouy-Maumus, G. J.; Clarke, T. B.; Edwards, A. M. Colistin Kills Bacteria by Targeting Lipopolysaccharide in the Cytoplasmic Membrane. *Elife* **2021**, *10*, e65836.
- (20) Ofek, I.; Cohen, S.; Rahmani, R.; Kabha, K.; Tamarkin, D.; Herzig, Y.; Rubinstein, E. Antibacterial Synergism of Polymyxin B Nonapeptide and Hydrophobic Antibiotics in Experimental Gram-Negative Infections in Mice. *Antimicrob. Agents Chemother.* **1994**, *38* (2), 374–377.
- (21) Vaara, M.; Vaara, T. Sensitization of Gram-Negative Bacteria to Antibiotics and Complement by a Nontoxic Oligopeptide. *Nature* **1983**, *303* (5917), 526–528.
- (22) Wesseling, C. M. J.; Slingerland, C. J.; Veraar, S.; Lok, S.; Martin, N. I. Structure–Activity Studies with Bis-Amidines That Potentiate Gram-Positive Specific Antibiotics against Gram-Negative Pathogens. *ACS Infect. Dis.* **2021**, *7*, 3314.
- (23) Tsubery, H.; Ofek, I.; Cohen, S.; Fridkin, M. Structure–Function Studies of Polymyxin B Nonapeptide: Implications to

Sensitization of Gram-Negative Bacteria. *J. Med. Chem.* **2000**, *43* (16), 3085–3092.

(24) Vaara, M. Polymyxin Derivatives That Sensitize Gram-Negative Bacteria to Other Antibiotics. *Molecules* **2019**, *24* (2), 249.

(25) Tsubery, H.; Ofek, I.; Cohen, S.; Eisenstein, M.; Fridkin, M. Modulation of the Hydrophobic Domain of Polymyxin B Nonapeptide: Effect on Outer-Membrane Permeabilization and Lipopolysaccharide Neutralization. *Mol. Pharmacol.* **2002**, *62* (5), 1036–1042.

(26) Siriwardena, T. N.; Gan, B. H.; Köhler, T.; van Delden, C.; Javor, S.; Reymond, J.-L. Stereorandomization as a Method to Probe Peptide Bioactivity. *ACS Cent. Sci.* **2021**, *7* (1), 126–134.

(27) Tsubery, H.; Ofek, I.; Cohen, S.; Fridkin, M. The Functional Association of Polymyxin B with Bacterial Lipopolysaccharide Is Stereospecific: Studies on Polymyxin B Nonapeptide. *Biochemistry* **2000**, *39* (39), 11837–11844.

(28) Vetterli, S. U.; Zerbe, K.; Müller, M.; Urfer, M.; Mondal, M.; Wang, S. Y.; Moehle, K.; Zerbe, O.; Vitale, A.; Pessi, G.; Eberl, L.; Wollscheid, B.; Robinson, J. A. Thanatin Targets the Intermembrane Protein Complex Required for Lipopolysaccharide Transport in *Escherichia Coli*. *Sci. Adv.* **2018**, *4* (11), eaau2634.

(29) Cochrane, S. A.; Findlay, B.; Vederas, J. C.; Ratemi, E. S. Key Residues in Octyl-Tridecapin A1 Analogues Linked to Stable Secondary Structures in the Membrane. *ChemBioChem.* **2014**, *15* (9), 1295–1299.

(30) Al Ayed, K.; Ballantine, R. D.; Hoekstra, M.; Bann, S. J.; Wesseling, C. M. J.; Bakker, A. T.; Zhong, Z.; Li, Y.-X.; Brüchle, N. C.; van der Stelt, M.; Cochrane, S. A.; Martin, N. I. Synthetic Studies with the Brevicidine and Laterocidine Lipopeptide Antibiotics Including Analogues with Enhanced Properties and in Vivo Efficacy. *Chem. Sci.* **2022**, *13* (12), 3563–3570.

(31) McDougal, P. G.; Griffin, J. H. Enantiotracin. *Bioorg. Med. Chem. Lett.* **2003**, *13* (13), 2239–2240.

(32) Kleijn, L. H. J.; Vlieg, H. C.; Wood, T. M.; Sastre Torano, J.; Janssen, B. J. C.; Martin, N. I. A High-Resolution Crystal Structure That Reveals Molecular Details of Target Recognition by the Calcium-Dependent Lipopeptide Antibiotic Laspartomycin C. *Angew. Chemie Int. Ed.* **2017**, *56* (52), 16546–16549.

(33) Moreira, R.; Taylor, S. D. The Chiral Target of Daptomycin Is the 2R,2'S Stereoisomer of Phosphatidylglycerol. *Angew. Chemie Int. Ed.* **2022**, *61* (4), e202114858.

(34) de Visser, P. C.; Kriek, N. M. A. J.; van Hooft, P. A. V.; Van Schepdael, A.; Filippov, D. V.; van der Marel, G. A.; Overkleeft, H. S.; van Boom, J. H.; Noort, D. Solid-Phase Synthesis of Polymyxin B1 and Analogues via a Safety-Catch Approach. *J. Pept. Res.* **2003**, *61* (6), 298–306.

(35) Gallardo-Godoy, A.; Muldoon, C.; Becker, B.; Elliott, A. G.; Lash, L. H.; Huang, J. X.; Butler, M. S.; Pelington, R.; Kavanagh, A. M.; Ramu, S.; Phetsang, W.; Blaskovich, M. A. T.; Cooper, M. A. Activity and Predicted Nephrotoxicity of Synthetic Antibiotics Based on Polymyxin B. *J. Med. Chem.* **2016**, *59* (3), 1068–1077.

(36) Moreira, R.; Barnawi, G.; Beriashvili, D.; Palmer, M.; Taylor, S. D. The Effect of Replacing the Ester Bond with an Amide Bond and of Overall Stereochemistry on the Activity of Daptomycin. *Bioorg. Med. Chem.* **2019**, *27* (1), 240–246.

(37) Danner, R. L.; Joiner, K. A.; Rubin, M.; Patterson, W. H.; Johnson, N.; Ayers, K. M.; Parrillo, J. E. Purification, Toxicity, and Antidotoxin Activity of Polymyxin B Nonapeptide. *Antimicrob. Agents Chemother.* **1989**, *33* (9), 1428–1434.

(38) Wood, T. M.; Slingerland, C. J.; Martin, N. I. A Convenient Chemoenzymatic Preparation of Chimeric Macrocyclic Peptide Antibiotics with Potent Activity against Gram-Negative Pathogens. *J. Med. Chem.* **2021**, *64* (15), 10890–10899.

(39) French, S.; Farha, M.; Ellis, M. J.; Sameer, Z.; Côté, J.-P.; Cotroneo, N.; Lister, T.; Rubio, A.; Brown, E. D. Potentiation of Antibiotics against Gram-Negative Bacteria by Polymyxin B Analogue SPR741 from Unique Perturbation of the Outer Membrane. *ACS Infect. Dis.* **2020**, *6* (6), 1405–1412.

(40) Jiang, X.; Sun, Y.; Yang, K.; Yuan, B.; Velkov, T.; Wang, L.; Li, J. Coarse-Grained Simulations Uncover Gram-Negative Bacterial Defense against Polymyxins by the Outer Membrane. *Comput. Struct. Biotechnol. J.* **2021**, *19*, 3885–3891.

(41) MacNair, C. R.; Stokes, J. M.; Carfrae, L. A.; Fiebig-Comyn, A. A.; Coombes, B. K.; Mulvey, M. R.; Brown, E. D. Overcoming *mcr-1* Mediated Colistin Resistance with Colistin in Combination with Other Antibiotics. *Nat. Commun.* **2018**, *9* (1), 458.

(42) Stokes, J. M.; MacNair, C. R.; Ilyas, B.; French, S.; Côté, J.-P.; Bouwman, C.; Farha, M. A.; Sieron, A. O.; Whitfield, C.; Coombes, B. K.; Brown, E. D. Pentamidine Sensitizes Gram-Negative Pathogens to Antibiotics and Overcomes Acquired Colistin Resistance. *Nat. Microbiol.* **2017**, *2* (5), 17028.

(43) Vaara, M. Agents That Increase the Permeability of the Outer Membrane. *Microbiol. Rev.* **1992**, *56* (3), 395–411.

(44) Helander, I. M.; Mattila-Sandholm, T. Fluorometric Assessment of Gram-Negative Bacterial Permeabilization. *J. Appl. Microbiol.* **2000**, *88* (2), 213–219.

(45) Martin, N. I.; Hu, H.; Moake, M. M.; Churey, J. J.; Whittall, R.; Worobo, R. W.; Vederas, J. C. Isolation, Structural Characterization, and Properties of Mattacin (Polymyxin M), a Cyclic Peptide Antibiotic Produced by *Paenibacillus kobensis* M. *J. Biol. Chem.* **2003**, *278* (15), 13124–13132.

(46) Brandenburg, K.; Arraiza, M. D.; Lehwerk-Ivetot, G.; Moriyon, I.; Zähringer, U. The Interaction of Rough and Smooth Form Lipopolysaccharides with Polymyxins as Studied by Titration Calorimetry. *Thermochim. Acta* **2002**, *394* (1), 53–61.

(47) Koch, P.-J.; Frank, J.; Schüler, J.; Kahle, C.; Bradaczek, H. Thermodynamics and Structural Studies of the Interaction of Polymyxin B with Deep Rough Mutant Lipopolysaccharides. *J. Colloid Interface Sci.* **1999**, *213* (2), 557–564.

(48) Odds, F. C. Synergy, Antagonism, and What the Chequerboard Tells between Them. *J. Antimicrob. Chemother.* **2003**, *52* (1), 1.

Recommended by ACS

Synthesis, Antibacterial Activity, and Nephrotoxicity of Polymyxin B Analogues Modified at Leu-7, d-Phe-6, and the N-Terminus Enabled by S-Lipidation

Paul W. R. Harris, Margaret A. Brimble, *et al.*

NOVEMBER 22, 2022
ACS INFECTIOUS DISEASES

READ 

Synthesis and Evaluation of Polymyxins Bearing Reductively Labile Disulfide-Linked Lipids

Cornelis J. Slingerland, Nathaniel I. Martin, *et al.*

NOVEMBER 18, 2022
JOURNAL OF MEDICINAL CHEMISTRY

READ 

Synthesis and Antimicrobial Evaluation of New Cephalosporin Derivatives Containing Cyclic Disulfide Moieties

Inga S. Shchelik and Karl Gademann

OCTOBER 17, 2022
ACS INFECTIOUS DISEASES

READ 

Cooperative Membrane Damage as a Mechanism for Pentamidine–Antibiotic Mutual Sensitization

Yu Zhou, Xinxin Feng, *et al.*

OCTOBER 21, 2022
ACS CHEMICAL BIOLOGY

READ 

Get More Suggestions >